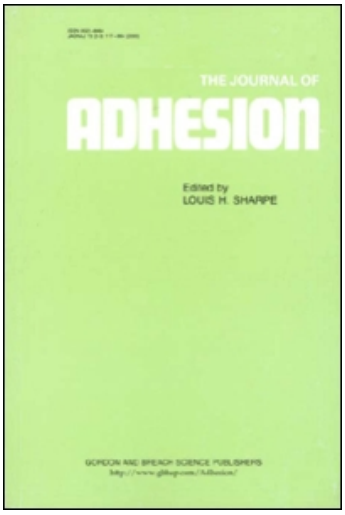

The Journal of Adhesion

Publication details, including instructions for authors and subscription information:
http://www.informaworld.com/smpp/title~content=t713453635

Peel Stress Distributions between Adherends with Varying Curvature Mismatch

Todd A. Corson[a]; Yeh-Hung Lai[a]; David A. Dillard[a]
[a] Engineering Science & Mechanics Department, Virginia Polytechnic Institute, Blacksburg, Virginia, U.S.A.

To cite this Article Corson, Todd A. , Lai, Yeh-Hung and Dillard, David A.(1990) 'Peel Stress Distributions between Adherends with Varying Curvature Mismatch', The Journal of Adhesion, 33: 1, 107 — 122
To link to this Article: DOI: 10.1080/00218469008030420
URL: http://dx.doi.org/10.1080/00218469008030420

J. Adhesion, 1990, Vol. 33, pp. 107–122
Reprints available directly from the publisher
Photocopying permitted by license only

Printed in the United Kingdom

Peel Stress Distributions between Adherends with Varying Curvature Mismatch†

TODD A. CORSON, YEH-HUNG LAI and DAVID A. DILLARD‡

Engineering Science & Mechanics Department, Virginia Polytechnic Institute, Blacksburg, Virginia 24061, U.S.A.

(Received December 18, 1989; in final form July 30, 1990)

Previously-derived, closed-form solutions for the residual peel stresses developed between adherends with a slight but constant curvature mismatch are extended to the cases of two or more discrete curvatures and continuously varying curvatures. This beam on elastic foundation solution is now used to predict, for example, the peel stresses which develop when a molding strip is bonded to conform to a substrate with varying curvatures. Diagrams of typical stress distributions are given along with plots which allow the designer to estimate or minimize the resulting peel stresses for specific applications.

KEY WORDS Beam on elastic foundation; curved adherends; molding strips; adhesive peel stresses

INTRODUCTION

When two adherends with an initial curvature mismatch are forced to conform to one another and then bonded with an adhesive layer, residual peel stresses result. Common examples from the automotive, aircraft, and construction industries include cases where flat molding strips are bonded to curved surfaces and where curved strips are forced onto flat substrates. The integrity and durability of these bonded structures will depend on the fracture resistance of the material system, and on the magnitude of the residual stresses. When bonding such components, an important design consideration should be the peel stresses which are induced along the bond due to the mismatch in curvature. This paper examines the stress distributions which result when there are discrete or continuously varying changes in the curvature mismatch between the adherends. The techniques developed herein are extensions of our earlier work[1] which addressed only the case of a constant mismatch in curvature. A closed-form solution for discrete curvature

† Presented at the Thirteenth Annual Meeting of The Adhesion Society, Inc., Savannah, Georgia, U.S.A., February 19–21, 1990.

‡ Corresponding author.

changes is presented herein for the case of two curvatures, and the development procedure is described for cases of more than two curvatures. One of the design uses of the technique is to find the optimal length to extend a molding strip past a curved surface onto a flat surface to reduce the likelihood of debonding. Analyses of this and other cases will be presented in the sample graphs section. In addition, the governing differential equation for cases where there is a continuously varying curvature mismatch is also presented. The closed form solution for the case of a sinusoidally varying mismatch is presented, and the process of using Fourier series expansions then to obtain the solution to arbitrary problems is discussed.

DEVELOPMENT OF BASIC FORMULATION

In order to develop the mathematical basis for the current method, it is advantageous to enhance the formulation and rigor of the approach we used in our previous technique. Some of the development will be identical to that used in Ref. 1, and the interested reader should refer to it for additional details.

The original technique was developed around the typical geometry shown in Figure 1 where an initially curved strip is bonded to a flat, rigid surface. (Figure 1 illustrates a positive curvature mismatch). The adhesive is assumed to be linearly elastic and the solution is based on a beam on elastic foundation analysis discussed in detail by Hetényi.[2] The bending stiffness of the strip is constant and is denoted by EI, where E is the elastic modulus of the material and I is the

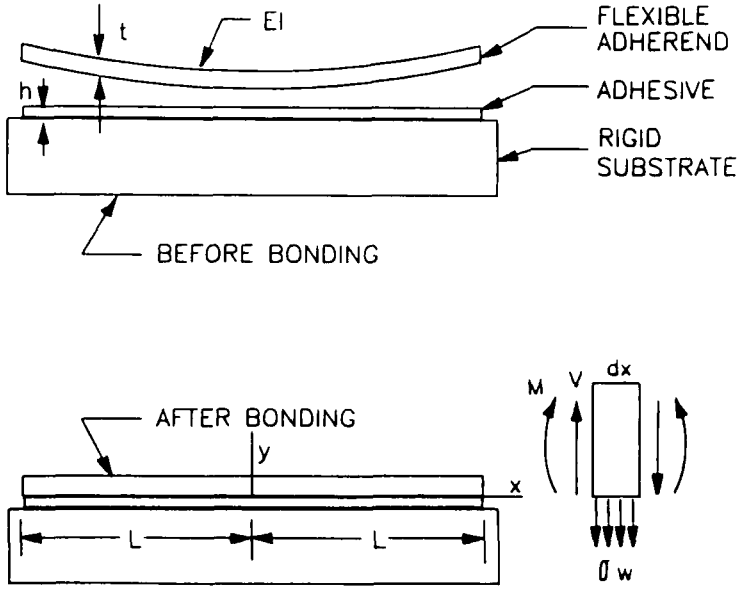

FIGURE 1 Sign conventions and dimensions for the analysis.

moment of inertia of the cross-section. The modulus of the adhesive is denoted by E_a, the thickness of the adhesive layer is h, and the width of the adhesive strip is w. The shear and bending moment conventions are as shown in Figure 1.

In general, the slopes involved in bending strips around curved substrates are not necessarily small, so in this paper we choose a curvilinear coordinate system in such a way that the instantaneous x-axis always coincides with the surface of the rigid substrate, and the y-axis is always perpendicular to this surface. A second curvilinear coordinate system is defined with the x_1 and y_1 axes parallel and perpendicular to the flexible adherend, as shown in Figure 2. We will require that the thickness of the flexible adherend is very small in comparison with the radius of curvature at every point along each surface so that simple beam theory will be applicable, but we make no other restrictions on the curvatures of the members. For convenience, we assume that the substrate is relatively rigid with respect to the strip, thus allowing the x and y axes to remain the same even after bonding has occurred. (If both adherends are flexible, the x and y axes should be selected so that they coincide with the deformed surface, and the effective EI of the system is the inverse of the sum of the individual compliances.[1]) The net curvature mismatch may be expressed as:

$$\frac{1}{\rho_0} = \frac{1}{\rho_a} - \frac{1}{\rho_b} \tag{1}$$

where ρ_a and ρ_b are the individual radii of curvatures of the two adherends, and the net curvature mismatch is the inverse of the effective (mismatched) radius of curvature, ρ_0.

We now elastically conform the strip to the substrate and assume it may be held in place by an adhesive layer which is also thin compared with the radii of curvature. Although the original slopes of strip and substrate may have been arbitrarily large, the choice of a curvilinear coordinate system allows us to assume, reasonably, that the slopes of the deformed strip will always be small with respect to the x-y coordinate system. This allows us now accurately to

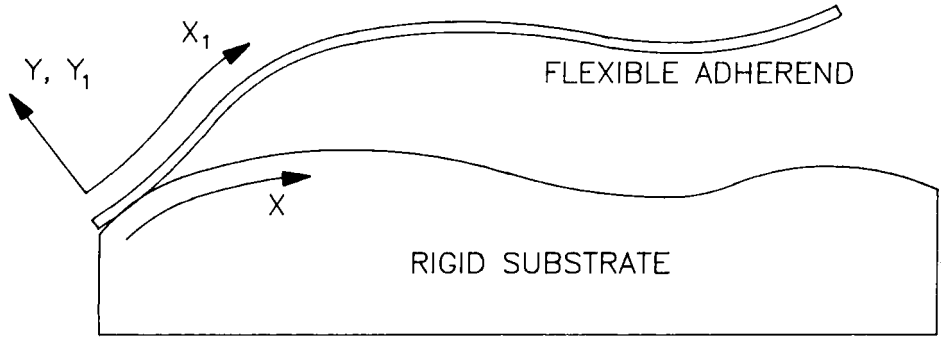

FIGURE 2 Curvilinear coordinate system used for the analysis of varying adherend curvature mismatch.

replace

$$\frac{1}{\rho}-\frac{1}{\rho_0}=\frac{M}{EI} \tag{2}$$

where M is the applied bending moment, ρ is the net radius of curvature of the deformed adherend, and ρ_0 is the stress free radius of curvature of the adherend, with

$$\frac{d^2}{dx^2}(y-y_0)=\frac{M}{EI} \tag{3}$$

Denoting the peel stress by $\sigma(x)$, and assuming as noted earlier that the adhesive is linear elastic, we obtain:

$$\sigma(x)=E_a\varepsilon=\frac{E_a}{h}y(x) \tag{4}$$

Using the elementary mechanics principle that the second derivative of the moment is the distributed force function, and substituting in Eq. (4), we have:

$$\frac{d^2M(x)}{dx^2}=-\frac{E_aw}{h}y(x) \tag{5}$$

Differentiating Eq. (3) twice and substituting in Eq. (5), we obtain:

$$\frac{d^4y}{dx^4}+4\lambda^4y=\frac{d^4y_0}{dx^4} \tag{6}$$

where:

$$\lambda=\left(\frac{E_aw}{4EIh}\right)^{1/4} \tag{7}$$

If the curvature mismatch is constant, the right hand side of Eq. (6) vanishes and the solution to this homogeneous fourth order equation is the standard beam on elastic foundation expression:

$$y(x)=e^{-\lambda x}(A\cos\lambda x+B\sin\lambda x)+e^{\lambda x}(C\cos\lambda x+D\sin\lambda x) \tag{8}$$

which is subject to the boundary conditions of no shear or moment at the ends:

$$M(-L)=M(L)=V(-L)=V(L)=0 \tag{9}$$

The coefficients can then be determined, and a closed form solution for peel stresses is obtained. Details for this derivation can be found in any advanced mechanics of materials text, such as Ref. 3, and specific information and graphs can be found once again in the previous paper.[1]

In applying these formulas to actual joints, it is useful to identify the functional dependency of the maximum peel stresses on the geometrical and material parameters. It may be easily shown that the maximum peel stress is proportional to $(E_a)^{1/2}$, $(E)^{1/2}$, and $(I)^{1/2}$, and is inversely proportional to $(h)^{1/2}$, $(w)^{1/2}$, and ρ. As pointed out by Reeves,[4] doubling the width of the adhesive layer does not

halve the peel stresses. The radicals on each of the quantities reflect the fact that altering the relative stiffness of the adhesive (by changing the geometry or material properties) will affect the stress distribution. Thus, increasing the adhesive width results in an increased area to share the load, but also draws higher loads because of the increased effective stiffness. Indeed, the most efficient means of reducing stresses would be preforming of the adherends to reduce the cuvature mismatch.

EXTENSION OF TECHNIQUE TO TWO CURVATURES

Using the general solution to the governing differential equation, we now extend the technique to two (or more) curvatures. Figure 3 shows the geometry we will use to develop our extended technique. Since the strip is composed of two curvatures, we will use one equation of the same form as Eq. (8) for each of its two sections as follows:

$$y_1(x) = e^{-\lambda x}(A_1 \cos \lambda x + B_1 \sin \lambda x) + e^{\lambda x}(C_1 \cos \lambda x + D_1 \sin \lambda x) \quad (10a)$$

$$y_2(x) = e^{-\lambda x}(A_2 \cos \lambda x + B_2 \sin \lambda x) + e^{\lambda x}(C_2 \cos \lambda x + D_2 \sin \lambda x) \quad (10b)$$

We now must solve for eight coefficients instead of four. We still have the four boundary conditions from the previous method (shear and moment equal zero at

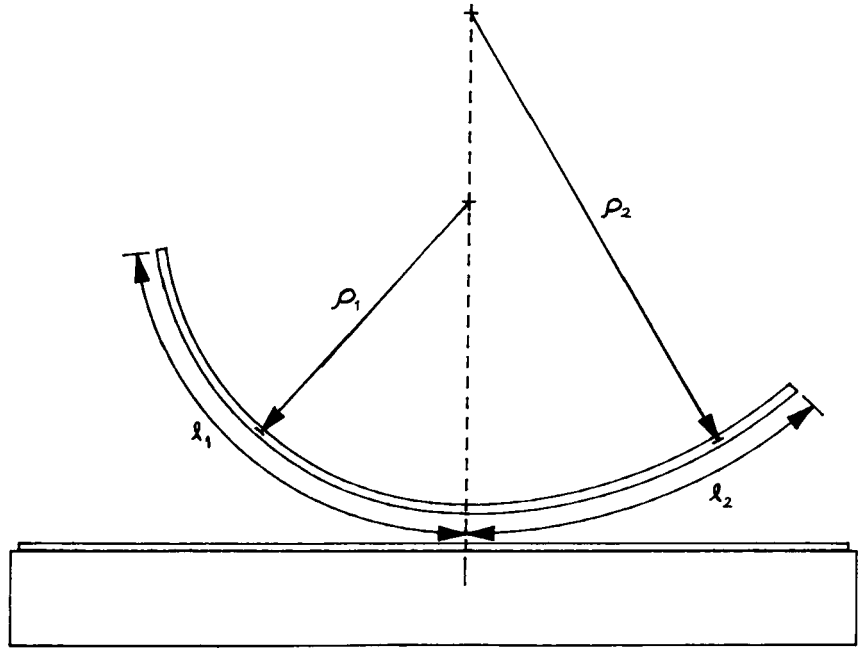

FIGURE 3 Geometry for the special case of two discrete curvatures.

ends). If we consider the origin to be at the change in curvature, these become:

$$M(-l_1) = M(l_2) = V(-l_1) = V(l_2) = 0 \tag{11}$$

which translate to:

$$\begin{aligned} y_1''(-l_1) &= \frac{1}{\rho_1} & y_2''(l_2) &= \frac{1}{\rho_2} \\ y_1'''(-l_1) &= 0 & y_2'''(l_2) &= 0 \end{aligned} \tag{12a}$$

($y'' = 1/\rho$ because when the moment is equal to zero, the curvature mismatch is equal to ρ.)

Now we must determine four more boundary conditions. These conditions can be obtained by matching displacement, slope, moment, and shear at the intersection of the two curvatures. We obtain:

$$\begin{aligned} y_1(0) &= y_2(0) & y_1'(0) &= y_2'(0) \\ y_1''(0) - \frac{1}{\rho_1} &= y_2''(0) - \frac{1}{\rho_2} & y_1'''(0) &= y_2'''(0) \end{aligned} \tag{12b}$$

thus fulfilling our need for eight boundary conditions. It is now possible to solve for the coefficients in Eqs. (10).

After close inspection one will find that solving for the coefficients by hand would be quite a task. Fortunately, computer programs have been developed for such occasions, and one of these programs was found invaluable in developing a closed-form solution for the two-curvature case. The program used was a symbolic algebra manipulator called MACSYMA.[5] The equations and boundary conditions were entered into the program, and the program solved for the eight coefficients. Very complicated expressions were obtained, were simplified using a few of the program's built in simplifying functions, and finally were reduced by hand into a useable form. The coefficients are presented in Appendix A.

If we examine these coefficients we see that we have terms inversely proportional to ρ_1 and ρ_2 and proportional to the difference over the product of the two curvatures. If one of the sections is flat (infinite curvature) or has a much larger radius of curvature than the other section, one of the terms drops out, and the term dependent on the difference becomes dependent only on the tightest curvature (smallest radius).

The first case we consider is to examine methods for reducing the peak peel stresses which develop due to a curvature mismatch. It is known that, for a constant curvature mismatch, the only peel stresses are those which develop locally at each end of the strip.[1] Presumably, these high peel stress concentrations could be reduced if the adherend curvature mismatch were reduced or eliminated at the very ends of the bondline. Figure 4 shows typical adhesive deformation distributions which are obtained when the curvature mismatch is eliminated for several different lengths. The data were obtained from the closed form solution where the curved length to the left is very long, and the zero mismatch region takes on increasing lengths. As the zero mismatch region vanishes, one regains

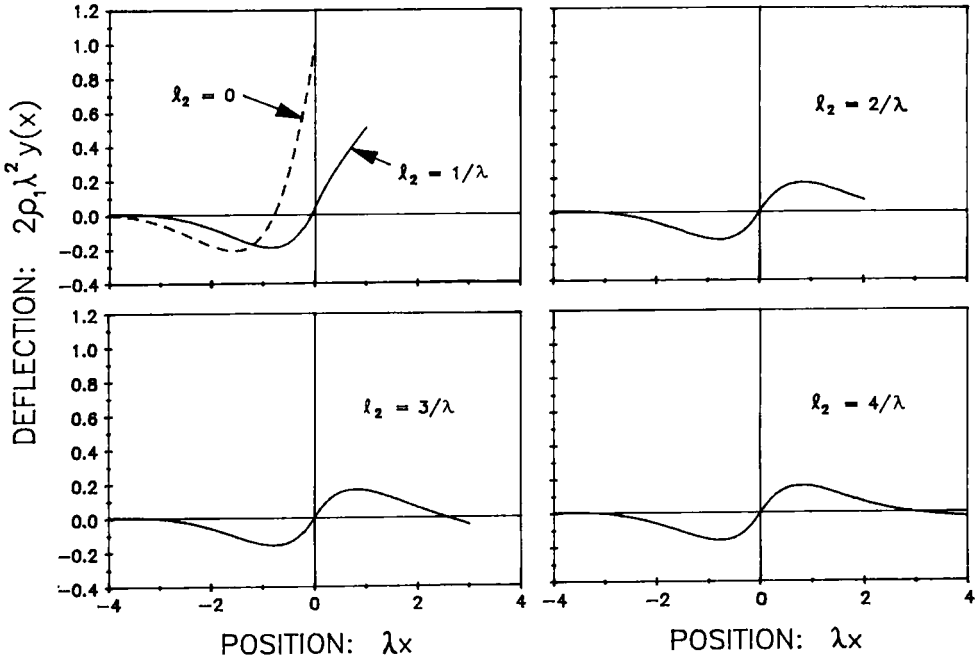

FIGURE 4 Deformation of the adhesive layer near the end of a constant curvature adherend with and without various length zero curvature mismatch terminal zones. (The curvature mismatch to the left of the origin is ρ_1, and the curvature mismatch to the right of the origin is zero.)

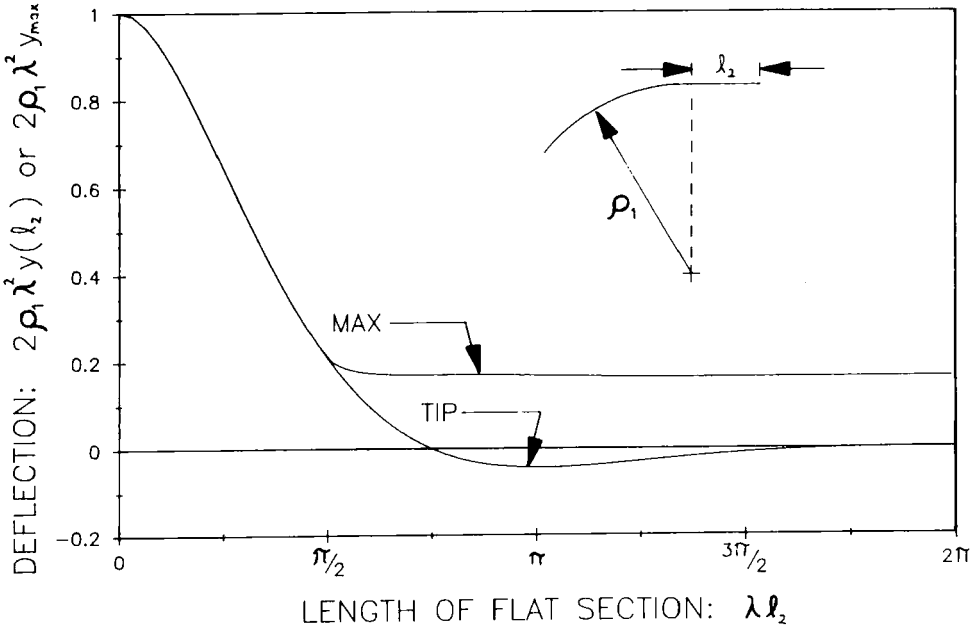

FIGURE 5 Maximum deformations in the adhesive layer as a function of length of a zero mismatch terminal zone.

the high stress concentrations obtained in Ref. 1. As the length of the zero mismatch region becomes large, a stable stress distribution which produces the couple needed to balance out the change in moment is produced. This configuration results in considerably smaller tensile stresses than the case where the curvature mismatch extends to the end of the adherend, and can also place the tip region in compression. Figure 5 is a summary graph of the tip and maximum displacements for various zero mismatch strip lengths. From a design standpoint, we note that if the curvature mismatch is eliminated over a region $l_2 = \pi/2\lambda$, the maximum peel stresses can be reduced to only 20% of the case with no zero mismatch terminal region. We can see the best length for a zero mismatch terminal region from a design standpoint is π/λ, since this gives us a maximum stress close to (approx. 2.7% greater than) the smallest obtainable, and the largest compressive tip stress. In this way, if any stresses are induced by moisture or temperature, we can still be fairly certain of a compressive stress at the tip of the bond, thus reducing the likelihood of peel initiation.

Figures 6 and 7 examine the stresses induced at the junction of two infinitely long sections of different curvatures. In order to normalize the results, we assume ρ_1 has the smaller radius of curvature. We obtain a family of graphs dependent on the ratio of the two curvatures as shown in Figure 6. The graphs is symmetrical about both axes, and is equivalent to a flat beam on an elastic foundation with a moment (equal to that needed to offset the change in curvature) applied at the

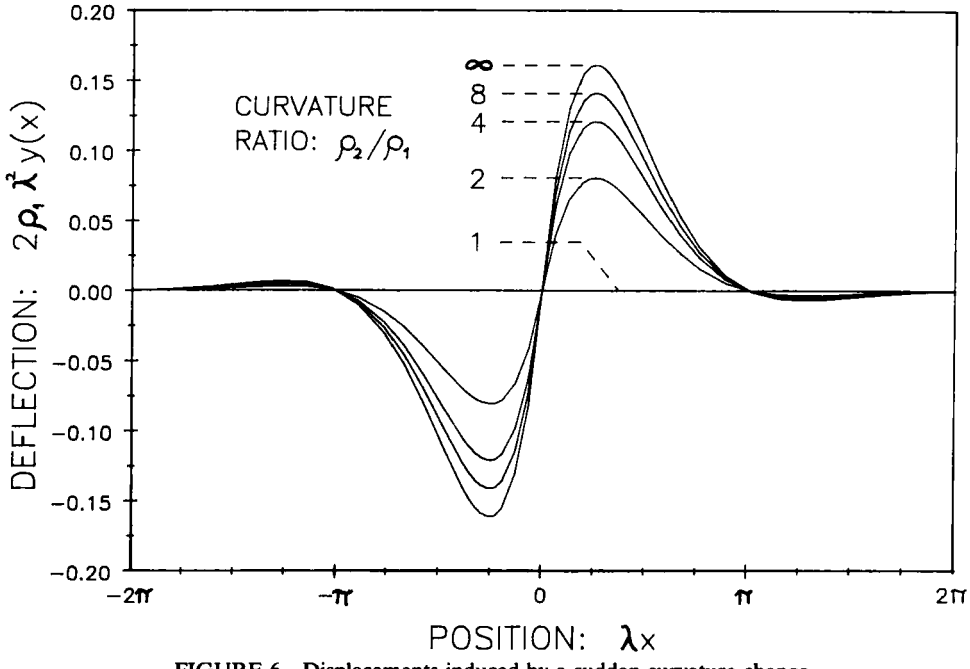

FIGURE 6 Displacements induced by a sudden curvature change.

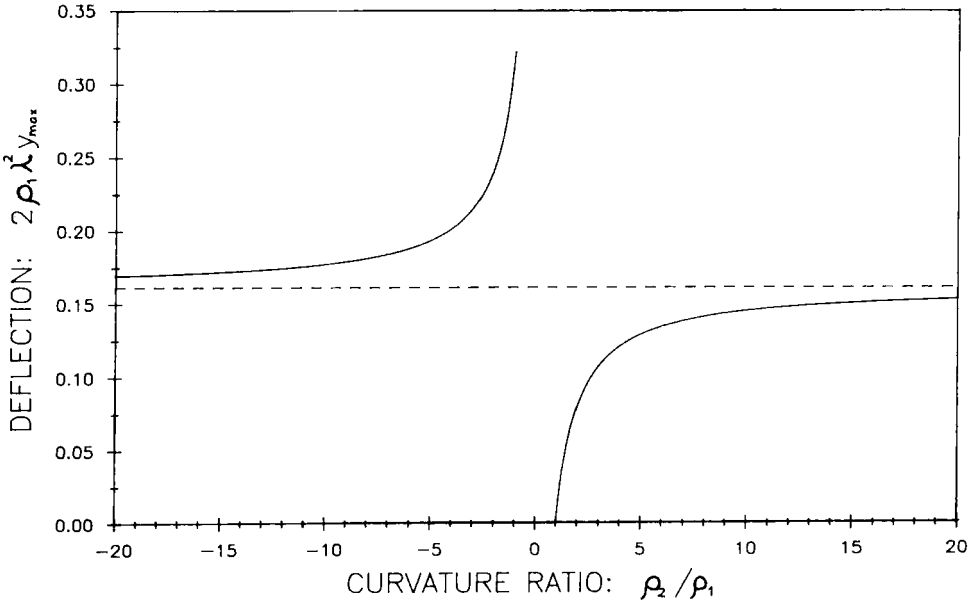

FIGURE 7 Maximum displacement induced by a sudden curvature change.

center. Figure 7 is a graph of the maximum displacements for various curvature ratios. For the case of a negative curvature ratio (the curvatures are in opposite directions) we simply note that a radius of $-\infty$ is equivalent to ∞. Then we add the stresses we would obtain from the cases of ρ_1 to ∞, and $-\infty$ to ρ_2 (assuming ρ_2 is the negative curvature). The tensile stress will always be on the side with the most negative curvature (flattest side if curvatures are of the same sign). It is also of interest to note that the maximum stresses are at a distance of $\pi/4\lambda$ from the center.

Note: The graphs are given in terms of displacement in order to normalize the results. If stress is needed, simply multiply the function by the E_a/h value for the specific problem.

TECHNIQUE FOR CONTINUOUSLY VARYING CURVATURES

In order to consider cases where the curvature varies continuously, we recognize that the governing differential equation (Eq. (6)) may become non-homogenous. If curvature remained constant, we differentiated twice and had a homogeneous equation. If $1/\rho(x)$ varies linearly, we have a continuously varying curvature, but note that after differentiating twice, we retain a homogeneous equation. This implies that for long strips with a curvature which varies linearly, there will be stresses near the ends. There will be no intermediate peel stresses arising because the solution remains homogeneous.

If the curvature varies in a more complex manner, we obtain a non-homogeneous differential equation:

$$y'''' + 4\lambda^4 y = y_0'''' \tag{13}$$

Solutions may be obtained by exact or numerical means for arbitrary curvature functions.

As an example, we choose the case of adherends with a sinusoidal mismatch given by:

$$y_0(x) = \hat{y}_0 \sin\left(\frac{2\pi x}{l}\right) \tag{14}$$

and for illustration purposes will assume that the bond line is long and that we are well away from the effects near the ends. We also assume that the amplitude of the sine wave is small in comparison with the period so that we can approximate the curvature by y_0''. Solving the governing differential equation, we obtain the peel stress distribution:

$$\sigma(x) = \hat{\sigma}_0 \sin\left(\frac{2\pi x}{l}\right) \tag{15}$$

where

$$\hat{\sigma}_0 = \left[\frac{1}{1 + 4\lambda^4 (l/2\pi)^4}\right] \frac{E_a}{h} \hat{y}_0 \tag{16}$$

We note that for the case where $\lambda \ll 2\pi/l$, the adherend is too stiff to conform to the closely spaced undulations, and

$$\sigma(x) = \hat{y}_0 \frac{E_a}{h} \sin\left(\frac{2\pi x}{l}\right) \tag{17}$$

implying that the deformation occurs in the adhesive rather than the adherends. If $\lambda \gg 2\pi/l$, the soft adherend readily conforms to the widely spaced undulations, and

$$\sigma(x) = \hat{y}_0 \frac{E_a}{4h} \left(\frac{2\pi}{\lambda l}\right)^4 \sin\left(\frac{2\pi x}{l}\right) \tag{18}$$

implying that the only stresses in the adhesive are those needed to induce the curvature. We note that these stresses decrease very rapidly as λ or l are increased. For cases where λ and $2\pi/l$ have similar magnitudes, Eq. (16) gives the stress distribution. The behavior near the ends can easily be determined by combining the homogeneous and particular solutions and imposing four boundary conditions of shear forces and bending moments at the ends being zero. The solution procedure and results are given in Appendix C.

TECHNIQUE FOR ADHERENDS OF ARBITRARY CURVATURES

The solition of the case of adherends with sinusoidal mismatch discussed in the previous section can also be easily extended to the case of adherends with

arbitrary curvatures by expressing y_0 as a Fourier series:

$$y_0(x) = \sum_{k=1}^{n} \left[a_k \sin\left(\frac{k\pi x}{L}\right) + b_k \cos\left(\frac{k\pi x}{L}\right) \right] \tag{19}$$

It should be noted that a finite number of terms could be chosen to approximate the initial mismatch of the adherends. The unknown coefficients A, B, C, and D in Eq. (8) can be determined by summing up as many coefficients obtained for the cases of $y_{0k}(x) = a_k \sin\left(\frac{k\pi x}{L}\right)$ and $y_{0k}(x) = b_k \cos\left(\frac{k\pi x}{L}\right)$ as chosen for Eq. 19. Once the unknown coefficients, A, B, C, and D, are determined, the deformed shape of adherend and stress distribution in the adhesive can be obtained. The advantage of this technique is that only four unknown coefficients need to be determined, which is easy and straightforward. It is only necessary to determine the initial adherend in the form of a Fourier series.

SUMMARY AND CONCLUSIONS

Residual peel stresses develop between adherends which initially have curvature mismatches. This paper and Ref. 1 have analyzed the distributions of these peel stresses which result when adherends with curvature mismatches are forced parallel and held together by an adhesive layer which was initially of uniform thickness. The analysis is based on an extension of the beam on elastic foundation solutions originally advanced by Winkler. For convenience, the analysis is based on the case of a flexible adherend bounded to a rigid substrate, although simple formulas are given in Ref. 1 to permit analysis when both adherends are flexible and curved. Slopes may be large prior to bonding, but radii of curvature must be large compared with the flexible adherend's height. Adherends and adhesive have been assumed to be elastic. Extensions of the solutions to cases with viscoelastic components are possible, but are complicated because of the multiple material system. Singularities at the bond termini have not been addressed, although the problem has also been couched from a fracture standpoint[1].

When the curvature mismatch is constant, and the bond length is long compared with $\frac{1}{\lambda} = \left(\frac{4EIh}{E_a w}\right)^{1/4}$, exponentially decaying sinusoidal peel stress distributions occur at the ends of the adherends, but rapidly dissipate away from the ends. For long bonds it can be shown that the strain energy release rate is given simply by $G = EI/2w\rho^2$, and is independent of debond length, thereby holding promise as a self-loading, constant strain energy release rate fracture test. (Kanninen[6] has shown that applying a couple to a bonded beam produces a constant strain energy release rate for the case of an externally applied moment, whereas we obtain the same result for an internally applied moment.) For convex facing (positive curvature mismatch) adherends, the maximum tensile peel stress occurs at the bond termini, and ignoring localized singularities, has a value of

$1/2\rho\lambda^2$. For concave facing (negative curvature mismatch) adherends, the maximum compressive stress has the same magnitude. The maximum tensile stress occurs inboard a distance of $\pi/2\lambda$, and is only approximately 20% of the maximum tensile stress for the positive curvature case. When an adherend mismatch is unavoidable, the adherends should be placed with concave sides facing whenever possible to take advantage of the reduced tensile stresses and possible reduction of bond terminus singularity effects.

The constant strain energy release rate property of this geometry implies that once a crack initiates, it will likely result in debonding of the majority of the bond length. It is only when the remaining bond length is smaller than approximately $3/\lambda$ that the strain energy release rate drops and continued fracture may be stopped. This implies that curved adherend bonds will debond for large distances, but remain intact over a small region, as has been experimentally observed.

For cases where the curvature changes abruptly from one constant curvature to a second constant curvature, peel stresses develop at this location to generate a couple which offsets the increased moment needed to deform the adherend. The magnitude of the peel stresses which result depends on the geometric and material properties of the system, and on the ratio of the radii of curvature. When the adherend extends only a short distance beyond the point of curvature change, the stress distributions of the end and junction can interfere with each other to produce distorted stress distributions. Improper dimensions can result in large tensile stresses, while dimensions can also be optimized to minimize the tensile stresses, or produce compressive stresses at the damage-prone ends.

By solving a nonhomogeneous differential equation, peel stress distributions for adherends with continuously varying curvatures can be determined. The case of a sinusoidal mismatch has been analyzed to illustrate the approach. The solution procedure for this case has also been extended to problems which have the forms of Fourier series. Thus, the problem of an arbitrarily varying curvature can also be solved analytically.

Acknowledgements

The authors would like to acknowledge the Adhesives & Sealants Council and the Center for Adhesive & Sealant Science and the National Science Foundation High Performance Polymeric Adhesives & Composities Science & Technology Center at Virginia Polytechnic Institute & State University for supporting one of the authors (TAC) as a 1989 ASC/CASS Summer Undergratuate Researcher.

References

1. D. A. Dillard, "Stresses between adherends with different curvatures", *J. Adhesion* **26**, 59–69 (1988).
2. M. Hetényi, *Beams on Elastic Foundations* (University of Michigan Press, Ann Arbor, 1946).
3. F. B. Seely and J. O. Smith, *Advanced Mechanics of Materials, 2nd ed.* (Wiley, New York, 1952).
4. Mark E. Reeves. Unpublished internal report, 3M Corporation, 1989.
5. *MACSYMA*. Computer software. Symbolics, Inc., 1986.
6. M. E. Kanninen, "An augmented double cantilever beam model for studying crack propagation and arrest", *International J. Fracture* **9** (1), 83–92 (1973).

APPENDIX A

Coefficients for Two-Curvature Solution

$$n_1 = \lambda l_1 \qquad n_2 = \lambda l_2$$

$$\Delta = 4\lambda^2\rho_1\rho_2 e^{2n_2+2n_1}[2\cos(2n_2+2n_1) + 2\cosh(2n_2+2n_1) - 4]$$

$$\begin{aligned}\Delta \cdot A_1 = {} & 2\rho_1 e^{n_2}\{\sin(n_2) + \cos(n_2) - e^{2n_2+2n_1}[\sin(n_2+2n_1) + \cos(n_2+2n_1) \\ & + 2\sin(n_2)]\} + 2\rho_2 e^{2n_2+n_1}\{\sin(2n_2+n_1) - \cos(2n_2+n_1) \\ & + 2\sin(n_1) - e^{2n_2+2n_1}[\sin(n_1) - \cos(n_1)]\} + (\rho_2-\rho_1)e^{2n_2}\{\cos(2n_2) \\ & + 1 - e^{2n_1}[\sin(2n_2+2n_1) + \sin(2n_2) - \cos(2n_2) + \sin(2n_1) \\ & + \cos(2n_1)] - e^{2n_2+2n_1}[\cos(2n_1)+1]\}\end{aligned}$$

$$\Delta \cdot A_2 = \Delta \cdot A_1$$

$$\begin{aligned}\Delta \cdot B_1 = {} & -2\rho_2 e^{2n_2+n_1}\{\sin(2n_2+n_1) + \cos(2n_2+n_1) - 2\cos(n_1) \\ & + e^{2n_2+2n_1}[\sin(n_1) + \cos(n_1)]\} + 2\rho_1 e^{n_2}\{\sin(n_2) - \cos(n_2) \\ & + e^{2n_2+2n_1}[\sin(n_2+2n_1) - \cos(n_2+2n_1) + 2\cos(n_2)]\} \\ & - (\rho_2-\rho_1)\{1 - e^{2n_2}[\sin(2n_2) - 1] + e^{2n_2+2n_1}[\cos(2n_2+2n_1) \\ & - \sin(2n_2) - \cos(2n_2) - \sin(2n_1) + \cos(2n_1) - 2] - e^{4n_2+2n_1}[\sin(2n_1)+1]\}\end{aligned}$$

$$\begin{aligned}\Delta \cdot B_2 = {} & -2\rho_2 e^{2n_2+n_1}\{\sin(2n_2+n_1) + \cos(2n_2+n_1) - 2\cos(n_1) \\ & + e^{2n_2+2n_1}[\sin(n_1) + \cos(n_1)]\} + 2\rho_1 e^{n_2}\{\sin(n_2) - \cos(n_2) \\ & + e^{2n_2+2n_1}[\sin(n_2+2n_1) - \cos(n_2+2n_1) + 2\cos(n_2)]\} \\ & + (\rho_2-\rho_1)e^{2n_2}\{\sin(2n_2) - 1 + e^{2n_1}[\cos(2n_2+2n_1) + \sin(2n_2) + \cos(2n_2) \\ & + \sin(2n_1) - \cos(2n_1) - 2] + e^{2n_2+2n_1}[\sin(2n_1)+1] + e^{2n_2+4n_1}\}\end{aligned}$$

$$\begin{aligned}\Delta \cdot C_1 = {} & 2\rho_2 e^{n_1}\{\sin(n_1) + \cos(n_1) - e^{2n_1+2n_2}[\sin(n_1+2n_2) \\ & + \cos(n_1+2n_2) + 2\sin(n_1)]\} + 2\rho_1 e^{2n_1+n_2}\{\sin(2n_1+n_2) - \cos(2n_1+n_2) \\ & + 2\sin(n_2) - e^{2n_1+2n_2}[\sin(n_2) - \cos(n_2)]\} + (\rho_1-\rho_2)e^{2n_1}\{\cos(2n_1) \\ & + 1 - e^{2n_2}[\sin(2n_1+2n_2) + \sin(2n_1) - \cos(2n_1) + \sin(2n_2) \\ & + \cos(2n_2)] - e^{2n_1+2n_2}[\cos(2n_2)+1]\}\end{aligned}$$

$$\Delta \cdot C_2 = \Delta \cdot C_1$$

$$\begin{aligned}\Delta \cdot D_1 = {} & 2\rho_1 e^{2n_1+n_2}\{\sin(2n_1+n_2) + \cos(2n_1+n_2) - 2\cos(n_2) \\ & + e^{2n_1+2n_2}[\sin(n_2) + \cos(n_2)]\} - 2\rho_2 e^{n_1}\{\sin(n_1) - \cos(n_1) \\ & + e^{2n_1+2n_2}[\sin(n_1+2n_2) - \cos(n_1+2n_2) + 2\cos(n_1)]\} \\ & - (\rho_1-\rho_2)e^{2n_1}\{\sin(2n_1) - 1 + e^{2n_2}[\cos(2n_1+2n_2) + \sin(2n_1) + \cos(2n_1) \\ & + \sin(2n_2) - \cos(2n_2) - 2] + e^{2n_1+2n_2}[\sin(2n_2)+1] + e^{2n_1+4n_2}\}\end{aligned}$$

$$\begin{aligned}\Delta \cdot D_2 = {} & 2\rho_1 e^{2n_1+n_2}\{\sin(2n_1+n_2) + \cos(2n_1+n_2) - 2\cos(n_2) \\ & + e^{2n_1+2n_2}[\sin(n_2) + \cos(n_2)]\} - 2\rho_2 e^{n_1}\{\sin(n_1) - \cos(n_1) \\ & + e^{2n_1+2n_2}[\sin(n_1+2n_2) - \cos(n_1+2n_2) + 2\cos(n_1)]\} \\ & + (\rho_1-\rho_2)\{1 - e^{2n_1}[\sin(2n_1) - 1] + e^{2n_1+2n_2}[\cos(2n_1+2n_2) - \sin(2n_1) \\ & - \cos(2n_1) - \sin(2n_2) + \cos(2n_2) - 2] - e^{4n_1+2n_2}[\sin(2n_2)+1]\}\end{aligned}$$

Note: C_1 can be obtained by switching the subscripts of all ρ's and n's in A_1. Also, D_1 is equal to $-B_2$ with its subscripts switched, and D_2 equals $-B_1$ with its subscripts switched. This result parallels that in the first paper (Ref. 1), where $C = A$ and $D = -B$.

APPENDIX B

Extension of Technique to Problems with Three of More Discrete Curvatures

In the same way that we extended the one-curvature problem to two curvatures, we can extend the two-curvature problem to three or more discrete curvatures. Each time we add a new section to the problem, we need four more boundary conditions. We obtain these by matching the conditions at the new intersection. For each section of curvature, we have a different equation, and it is most convenient to have each section start at 0 and go to l_n. The conditions can be solved for a specific case using a computer, and the stresses can be graphed. For the n-curvature case, we have:

y_1	y_2	$\cdots$	y_{n-1}	y_n
ρ_1	ρ_2	$\cdots$	ρ_{n-1}	ρ_n
0 to l_1	0 to l_2		0 to l_{n-1}	0 to l_n

End conditions:

$$\begin{aligned} y_1''(0) &= \frac{1}{\rho_1} & y_1'''(0) &= 0 \\ y_n''(l_n) &= \frac{1}{\rho_n} & y_n'''(l_n) &= 0 \end{aligned} \tag{B1}$$

Intersection conditions:

$$\begin{aligned} y_1(l_1) &= y_2(0) & y_1'(l_1) &= y_2'(0) \\ y_1''(l_1) - \frac{1}{\rho_1} &= y_2''(0) - \frac{1}{\rho_2} & y_1'''(l_1) &= y_2'''(0) \end{aligned} \tag{B2}$$

$$\vdots$$

$$\begin{aligned} y_{n-1}(l_{n-1}) &= y_n(0) & y_{n-1}'(l_{n-1}) &= y_n'(0) \\ y_{n-1}''(l_{n-1}) - \frac{1}{\rho_{n-1}} &= y_n''(0) - \frac{1}{\rho_n} & y_{n-1}'''(l_{n-1}) &= y_n'''(0) \end{aligned} \tag{B3}$$

Stress distributions for the multiple curvature case can also be obtained by combining sections of two curvatures when the separation between curvature changes is sufficiently long. A good approximation can be obtained when each curvature change is at least $10/\lambda$ units away from the ends and other changes. The graphs combined to form each section of this approximation should be two infinite lengths of the proper curvature, and the center of this graph should be used for the approximation. This section should extend half way from the change to the end or the next change. The ends should be taken from the end of an

infinite length of the corresponding curvature. This technique will give more accurate results as the distances between curvature changes increase, but the multiple curvature technique will be accurate in any case.

APPENDIX C

The Solution for the Case of Adherends with a Sinusoidal Mismatch

From Eq. (14), the complete solution for the current case is given as:

$$y(x) = y_h(x) + y_p(x) \tag{C1-1}$$

where

$$y_p(x) = \frac{\hat{y}_0}{1 + 4\lambda^4[l/2\pi]^4} \sin\frac{2\pi x}{l} \tag{C1-2}$$

and $y_h(x)$ is the same as that in Eq. (8).

By imposing boundary conditions, $M(0) = M(L) = V(0) = V(L) = 0$, four linear equations are obtained:

$$y_n''(0) = \frac{1}{\rho_0(0)} - y_p''(0), \tag{C2-1}$$

$$y_n''(L) = \frac{1}{\rho_0(L)} - y_p''(L), \tag{C2-2}$$

$$y_h'''(0) = \frac{d}{dx}\left(\frac{1}{\rho_0(x)}\right)\bigg|_{x=0} - y_p'''(0), \tag{C2-3}$$

$$y_h'''(L) = \frac{d}{dx}\left(\frac{1}{\rho_0(x)}\right)\bigg|_{x=L} - y_p'''(L). \tag{C2-4}$$

where

$$\frac{1}{\rho_0(x)} = -\frac{4\pi^2\hat{y}_0}{l^2}\sin\frac{2\pi x}{l}. \tag{C2-5}$$

By representing the known quantities on the right hand side of Eqs. (C2-1) through (C2-4) as k_1, k_2, k_3, and k_4, and solving this system of four linear simultaneous equations, we can obtain A, B, C, and D as follows:

$$\begin{aligned} A = &-\{e^{2\lambda L}[k_3(\sin(2\lambda L) + 1) + k_1\lambda(\cos(2\lambda L) - \sin(2\lambda L))] \\ &+ [(3k_2\lambda - 2k_4)e^{3\lambda L} - k_2\lambda e^{\lambda L}]\sin\lambda L + [(k_2\lambda + k_4)e^{3\lambda L} \\ &+ (-k_2\lambda - k_4)e^{\lambda L}]\cos\lambda L + (-k_1\lambda - k_3)e^{4\lambda L}\}/\Phi, \end{aligned} \tag{C3-1}$$

$$\begin{aligned} B = &\{e^{2\lambda L}[k_1\lambda(-\sin(2\lambda L) - \cos(2\lambda L) + 2) + k_3(\cos(2\lambda L) - 1)] \\ &+ [(k_2\lambda - k_4)e^{3\lambda L} + (k_2\lambda + k_4)e^{\lambda L}]\sin\lambda L \\ &+ [k_2\lambda(e^{3\lambda L} - e^{\lambda L})]\cos\lambda L - k_1\lambda e^{4\lambda L}]\}/\Phi, \end{aligned} \tag{C3-2}$$

$$C = -\{e^{2\lambda L}[k_1\lambda(\sin(2\lambda L) + \cos(2\lambda L)) + k_3(\cos(2\lambda L) - 1)] + [k_2\lambda e^{3\lambda L} + (-3k_2\lambda - 2k_4)e^{\lambda L}] \sin \lambda L + [-(k_2\lambda - k_4)e^{3\lambda L} + (k_2\lambda - k_4)e^{\lambda L}] \cos \lambda L - k_1\lambda + k_3\}/\Phi, \quad \text{(C3-3)}$$

$$D = \{e^{2\lambda L}[k_1\lambda(-\sin(2\lambda L) + \cos(2\lambda L) - 2) + k_3(\cos(2\lambda L) - 1)] + [(k_2\lambda - k_4)e^{3\lambda L} + (k_2\lambda + k_4)e^{\lambda L}] \sin \lambda L + [k_2\lambda(e^{3\lambda L} - e^{\lambda L})] \cos \lambda L + k_1\lambda\}/\Phi, \quad \text{(C3-4)}$$

where

$$\Phi = 2\lambda^3[e^{2\lambda L}(2\cos(2\lambda L) - 4) + e^{4\lambda L} + 1]. \quad \text{(C3-5)}$$

By substituting the above coefficients back into Eq. (C1-1) and Eq. (4), we could obtain the deformed adherend and stress distribution in the adhesive. It should be noted that for an initial adherend mismatch obeying a cosin function, $\cos\left(\frac{2\pi x}{l}\right)$, the solution could be obtained by replacing $\sin\left(\frac{2\pi x}{l}\right)$ with $\cos\left(\frac{2\pi x}{l}\right)$ in Eqs. (C1-2) and (C2-5). In addition, in order to calculate A, B, C, and D for $\cos\left(\frac{k\pi x}{L}\right)$ and $\sin\left(\frac{k\pi x}{L}\right)$ for an aherend with arbitrary initial shape expressed as a Fourier series, we could simply replace $\frac{2\pi x}{l}$ in Eqs. (C2-1) and (C2-5) with $\frac{k\pi x}{L}$.